

## Effects of sodium tungstate on characteristics of microarc oxidation coatings formed on magnesium alloy in silicate-KOH electrolyte

DING Jun(丁 军)<sup>1,2</sup>, LIANG Jun(梁 军)<sup>1,2</sup>, HU Li-tian(胡丽天)<sup>1</sup>, HAO Jing-cheng(郝京诚)<sup>1</sup>, XUE Qun-ji(薛群基)<sup>1</sup>

1. State Key Laboratory of Solid Lubrication, Lanzhou Institute of Chemical Physics, Chinese Academy of Sciences, Lanzhou 730000, China;

2. Graduate School of Chinese Academy of Sciences, Beijing 100039, China

Received 30 August 2006; accepted 12 January 2007

**Abstract:** Oxide coatings on AM60B magnesium alloy were prepared using the microarc oxidation(MAO) technique in silicate-KOH electrolyte with addition of 0–6.0 g/L Na<sub>2</sub>WO<sub>4</sub>. The MAO processes in base electrolyte with different concentrations of Na<sub>2</sub>WO<sub>4</sub> were studied. The microstructure, compositions and mechanical tribological characteristics of the oxide coatings were also investigated by SEM, XRD, XPS, microhardness analysis and ball-on-disc friction testing, respectively. It is found that the addition of Na<sub>2</sub>WO<sub>4</sub> into the base electrolyte has direct effect on the characteristics of voltage—time curves and breakdown voltage in MAO process. The number of micropores at top of the coating surface is increased by the addition of Na<sub>2</sub>WO<sub>4</sub>. The fraction of forsterite Mg<sub>2</sub>SiO<sub>4</sub> in the oxide coating increases with increasing concentration of Na<sub>2</sub>WO<sub>4</sub> in base electrolytes. Furthermore, the microhardness and wear resistance of oxide coatings are enhanced as well.

**Key words:** magnesium alloy; microarc oxidation; Na<sub>2</sub>WO<sub>4</sub>; oxide coating; wear resistance

### 1 Introduction

Magnesium alloys have high ratio of strength to mass, high dimensional stability, good electromagnetic shielding and damping characteristics, and are easy to machine and recycle. Thus its application is becoming attractive in a wide range of industries in recent years, especially in the fields where reduction is critical or particular technical requirements are needed, including automotive, aerospace and communication fields[1]. However, the main factors limiting the application of Mg alloys are their comparatively low corrosion and wear resistance[2]. Therefore, it is necessary to improve wear and corrosion resistance if magnesium is to be used for more industries fields. There are a number of possible coating technologies available for magnesium and its alloy including electrochemical plating, conversion coatings, anodizing, gas-phase deposition processes, laser surface alloying and organic coatings[3]. Among these techniques, anodizing is one of the most popular methods[4–7]. Microarc oxidation(MAO), as a relatively new surface treatment technique based on the traditional

anodizing process, has attracted great interest in recent years, because the oxide coating produced by MAO process is of excellent properties like anti-abrasion, corrosion resistance or decorative property on Al, Mg and Ti alloys and has promising application prospect in many fields[8–11].

It is found that the electrolyte compositions play a key role in the MAO process[12] and some of the polyvalent metal anions, such as chromate, tungstate, molybdate and vanadate, favor the microarc oxidation process and are promising for the formation of coatings of diverse chemical compositions[13]. The influence of polyvalent metal anions on the characteristics of MAO coatings on aluminum and titanium has been studied [14–17]. However, there is little research work with MAO process on magnesium alloy with addition of polyvalent metal anions in the base electrolyte. In this investigation, thus, the sodium tungstate was added to modify the base silicate-KOH electrolyte to obtain oxide coatings on magnesium alloy using the MAO process. The microstructure, composition and wear resistance of the oxide coatings formed in base electrolyte with addition of different concentrations of Na<sub>2</sub>WO<sub>4</sub> were

studied.

## 2 Experimental

### 2.1 Preparation of microarc oxidation coatings

Panel substrates made of the AM60B Mg alloy with a size of 20 mm×36 mm×2 mm (mass fraction: Al 5.6%–6.4%, Mn 0.26%–0.4%, Zn≤0.2%, balance Mg) were ground and polished with SiC abrasive paper to obtain an average surface roughness  $R_a \approx 0.18 \mu\text{m}$ . The base electrolyte was prepared from solution of sodium silicate (10.0 g/L) and potassium hydroxide (1.0 g/L) in distilled water. The MAO processes were carried out in the base electrolyte with addition of 0–6.0 g/L  $\text{Na}_2\text{WO}_4$ , using a bi-polar pulsed electrical source. The conductivity of the electrolytes was determined on an MC226 conductivity meter (Mettler-Toledo, Germany) and the breakdown voltage was obtained in different electrolytes using the appearance of the visible sparks as criterion for identifying the breakdown voltage. The averaged current density on the sample surface was predefined as  $J=6.0 \text{ A/dm}^2$  and maintained the cathodic current ( $I_c$ ) equal to the anodic current ( $I_a$ ), namely  $I_c/I_a=1$  by modulating the positive and negative voltage. The concentration of  $\text{Na}_2\text{WO}_4$ , electrolyte conductivity, the relevant breakdown voltage and the final voltage with the concentration of  $\text{Na}_2\text{WO}_4$  are listed in Table 1. The temperature of the electrolytes was always kept at 25–30 °C in the whole process. After MAO treatment, the coated samples were rinsed thoroughly in water and dried in warm air.

**Table 1** MAO process parameters at different concentrations of  $\text{Na}_2\text{WO}_4$  in silicate-KOH electrolytes

Concentration of $\text{Na}_2\text{WO}_4/(\text{g}\cdot\text{L}^{-1})$	Conductivity/ ( $\text{S}\cdot\text{m}^{-1}$ )	Breakdown voltage/V	Final voltage/V
0	1.29	200	505
2.0	1.31	180	490
4.0	1.40	155	485
6.0	1.44	135	480

### 2.2 Coating structure and composition analysis

A JSM-5600LV scanning electron microscope (SEM) was used to observe the surface morphology of the oxide coatings. The phase composition of the oxide coatings was studied by X-ray diffraction (XRD, X'Pert PRO), using  $\text{Cu K}\alpha$  radiation as the excitation source at a grazing angle of 2°. The XPS analyses of the oxide coatings were performed on a PHI-5702 multi-functional X-ray photoelectron spectroscope, using  $\text{Al K}\alpha$  radiation as the excitation source.

### 2.3 Mechanical and tribological evaluation

After the outer porous layer of the oxide coatings

was removed by abrasion against SiC paper, the microhardness was evaluated by means of a MH-5 hardness tester with a Vicker indenter at a load of 0.25 N for a loading duration of 5 s. The friction and wear properties of the oxide coatings were evaluated on a UMT-2MT reciprocal-sliding test rig sliding against  $\text{Si}_3\text{N}_4$  ball with a diameter of 3 mm in a ball-on-disc configuration. The unlubricated sliding was performed at a load of 2 N, a sliding speed of 0.1 m/s, sliding amplitude of 5 mm, and sliding duration of 30 min in ambient conditions of temperature and humidity. A computer connected to the tester recorded the friction coefficient curves and a friction coefficient was given at the end of the sliding test. Wear rates of oxide coatings were calculated by measuring the worn scar cross-sectional area of the sample with a profilometer.

## 3 Results and discussion

### 3.1 Voltage—time curves and breakdown voltage in microarc oxidation process

The oxide coatings are grown on magnesium alloy at a current density of  $6.0 \text{ A/dm}^2$  in 0, 2.0, 4.0 and 6.0 g/L  $\text{Na}_2\text{WO}_4$  aqueous solutions of silicate-KOH, respectively. Fig.1 shows the dependencies of the averaged positive and negative pulsed voltages on the oxidation time.

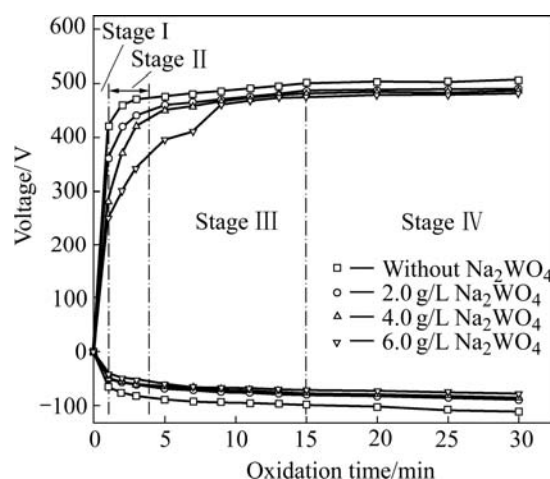


**Fig.1** Variation of voltages with oxidation time in silicate-KOH electrolyte with addition of different concentrations of  $\text{Na}_2\text{WO}_4$

According to the curves, four stages can be identified in all electrolytes. During the first 50–60 s (stage I), the voltages increase linearly with the oxidation time on the constant rate. In this stage, it is seen that the Mg alloy substrate is firstly dissolved and lost metal brightness, subsequently a thin barrier layer is formed on the sample surface. When the voltage exceeds the critical voltage of initial barrier layer, the small micro-sparks uniformly distributed on the sample surface

can be observed. In stage II, the rate of voltage increase diminishes. However, the micro-sparks on the sample surfaces become more and larger than those in stage I. It is also noted that the temporal duration of stage II lengthens with increasing concentration of  $\text{Na}_2\text{WO}_4$  in base electrolyte. After around 5–8 min of treatment, the processes enter stage III and the slope of the curve  $U=f(t)$  becomes smaller than that in stage II, where the appearance of the micro-sparks becomes more pronounced. Contrary to the stage II, the duration of stage III is obviously shortened with increasing concentration of  $\text{Na}_2\text{WO}_4$ , and even in the electrolyte containing 6.0 g/L  $\text{Na}_2\text{WO}_4$ , the stage III becomes evidently transitory. Further MAO processing makes the voltage enter more steady-state and some of the micro-sparks on the sample surfaces progress gradually from a dense population of small and frequent micro-sparks towards smaller populations of larger, slower moving and longer-lived discharge events, which becomes a major feature of the process in stage IV. But some small micro-sparks still exist between the larger micro-sparks. Comparing with all the voltage—time curves, it is found that the working voltage and final voltage decrease with increasing concentration of  $\text{Na}_2\text{WO}_4$  in the electrolytes. Furthermore, the number of small micro-sparks on the sample surface during the stage IV increases with increasing concentration of  $\text{Na}_2\text{WO}_4$ .

During the microarc oxidation process, dielectric breakdown occurs when the applied voltage exceeds the breakdown voltage of the initial barrier layer on substrate and a number of micro-sparks appear on the surface of the sample. The breakdown voltage has a strong dependence on the electrolytic composition and conductivity[18–19]. IKONOPISOV[18] proposed a theoretical model of breakdown caused by an avalanche of electrons injections at the electrolyte/oxide interface. According to this model, the breakdown voltage is related to the electrolyte conductivity as the following equation:

$$U_B = a_B + b_B \lg(1/\gamma) \quad (1)$$

where  $a_B$  and  $b_B$  are constants for a given metal and electrolyte composition,  $U_B$  and  $\gamma$  are the breakdown voltage and electrolyte conductivity, respectively.

As shown in Table 1, the breakdown voltage decreases with increasing concentration of  $\text{Na}_2\text{WO}_4$  in the silicate-KOH electrolyte and the electrolyte conductivity. A plot of breakdown voltage vs the logarithm of reciprocal of electrolyte conductivity ( $1/\gamma$ ) is shown in Fig.2. It is clear that this plot is approximately linear represented in Eqn.(1), which indicates that the breakdown mechanism of the initial barrier layer conforms to the model proposed by IKONOPISOV[18]

and the addition of  $\text{Na}_2\text{WO}_4$  in the silicate-KOH electrolyte can make the breakdown voltage decrease effectively.

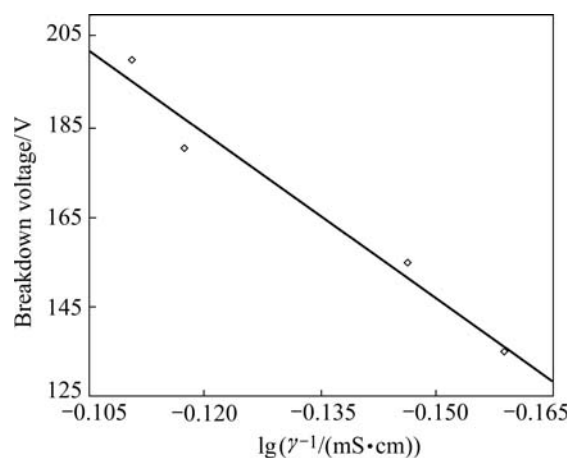


**Fig.2** Dependence of  $U_B$  on  $\lg(1/\gamma)$  during microarc oxidation of Mg alloy in silicate-KOH electrolytes with addition of different concentrations of  $\text{Na}_2\text{WO}_4$

### 3.2 Effect of $\text{Na}_2\text{WO}_4$ on composition and structure of microarc oxidation coatings

Fig.3 shows the morphologies of the oxide coatings formed in the silicate-KOH electrolyte with and without addition of  $\text{Na}_2\text{WO}_4$ . It is clear that the introduction of  $\text{Na}_2\text{WO}_4$  into the base electrolyte makes a significant change in the surface structure of the oxide coatings. In  $\text{Na}_2\text{WO}_4$ -free base electrolyte, the SEM image exhibits the appearance of repeated and concentrated sintering (Fig.3(a)). At top of the surface, some micropores exist in the coating. The diameter of the micropores ranges from 1 to 10  $\mu\text{m}$ . By comparison with the micrograph of Fig.3(a), the surfaces of the oxide coatings formed in the electrolytes with  $\text{Na}_2\text{WO}_4$  addition (Figs.3(b)–(d)) exhibit the looser and more porous microstructure. The coatings formed in the electrolyte containing  $\text{Na}_2\text{WO}_4$  have more micropores than that formed in the base electrolyte. Furthermore, the number of micropores increases with increasing concentration of  $\text{Na}_2\text{WO}_4$ , which may be attributed to that the fraction of smaller micro-sparks on the sample surface during the stage IV increases with increasing concentration of  $\text{Na}_2\text{WO}_4$  as mentioned above. In accordance with the changes of surface morphology, the surface roughness of the oxide coatings increases (see Table 2). In addition, as for the macroscopic appearance, it is found that the color of coating surface is also changed with addition  $\text{Na}_2\text{WO}_4$  into the electrolyte as described in Table 2. The color of coating surface changes from white to grey, and then to black with increasing concentration of  $\text{Na}_2\text{WO}_4$  in base electrolyte.

The XRD patterns for the oxide coatings formed in silicate-KOH electrolyte with addition of different

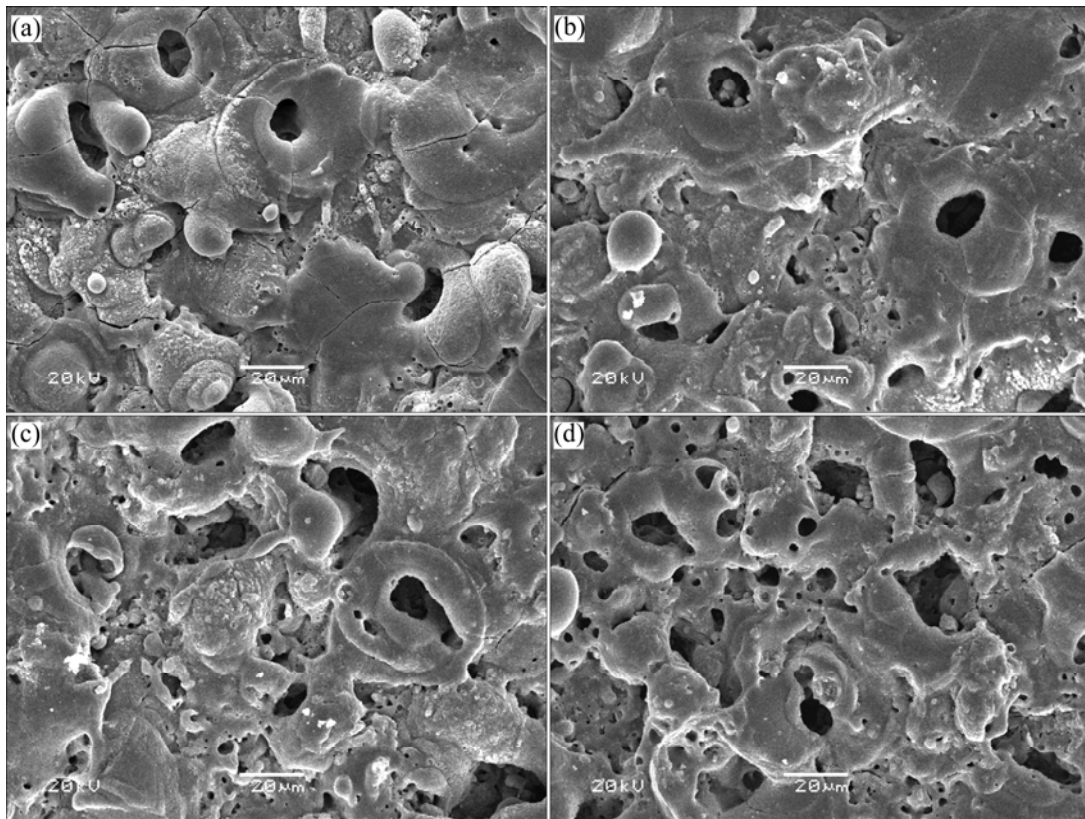


**Fig.3** Surface morphologies of oxide coatings formed in silicate-KOH electrolytes with addition of different concentrations of  $\text{Na}_2\text{WO}_4$ : (a) Without  $\text{Na}_2\text{WO}_4$ ; (b) 2.0 g/L  $\text{Na}_2\text{WO}_4$ ; (c) 4.0 g/L  $\text{Na}_2\text{WO}_4$ ; (d) 6.0 g/L  $\text{Na}_2\text{WO}_4$

**Table 2** Properties of oxide coatings formed in silicate-KOH electrolytes with addition of different concentrations of  $\text{Na}_2\text{WO}_4$

Concentration of $\text{Na}_2\text{WO}_4/(\text{g}\cdot\text{L}^{-1})$	Surface roughness/ $\mu\text{m}$	Microhardness, HV	Friction coefficient	Wear rate/ $(10^{-5}\text{mm}^3\cdot\text{N}^{-1}\cdot\text{m}^{-1})$	Color of coating surface
0	2.24	510	0.75	3.55	White
2.0	2.89	544	0.75	3.31	Grey
4.0	3.11	688	0.74	2.73	Dark grey
6.0	3.27	711	0.73	2.54	Black

concentrations of  $\text{Na}_2\text{WO}_4$  are shown in Fig.4. The XRD patterns clearly show that the periclase MgO and forsterite  $\text{Mg}_2\text{SiO}_4$  are the main compounds existing on the oxide coating, regardless of the electrolyte compositions. The oxide coating obtained in the base electrolyte without addition of  $\text{Na}_2\text{WO}_4$  consists mostly of MgO and the peaks of forsterite  $\text{Mg}_2\text{SiO}_4$  are lower. However, when AM60B Mg alloy is oxidized in the electrolyte containing  $\text{Na}_2\text{WO}_4$ , the peaks of forsterite  $\text{Mg}_2\text{SiO}_4$  are evidently enhanced in the XRD patterns. The relative content of MgO and  $\text{Mg}_2\text{SiO}_4$  in the coating can be judged based on the intensities of the strongest peaks corresponding to MgO(200) and  $\text{Mg}_2\text{SiO}_4$ (211) planes with similar interplanar distance (i.e. 0.210 6 nm and 0.216 0 nm, respectively) in XRD patterns[20–21] and the results shown in table inset in Fig.4. It can be seen that the addition of  $\text{Na}_2\text{WO}_4$  decreases evidently the fraction of periclase MgO and increases the fraction of

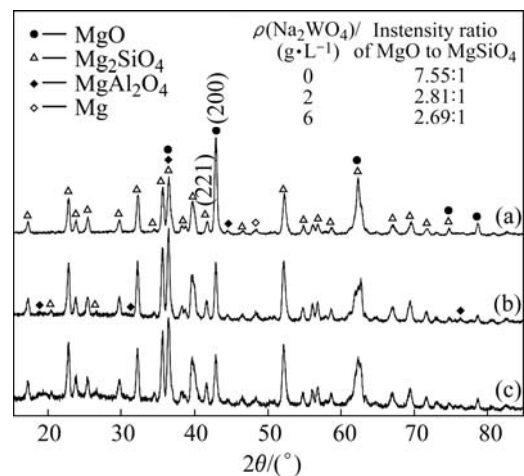


**Fig.4** XRD patterns of oxide coatings formed in silicate-KOH electrolyte with addition of different concentrations of  $\text{Na}_2\text{WO}_4$ : (a) Without  $\text{Na}_2\text{WO}_4$ ; (b) 2.0 g/L  $\text{Na}_2\text{WO}_4$ ; (c) 6.0 g/L  $\text{Na}_2\text{WO}_4$

forsterite  $Mg_2SiO_4$  in the oxide coatings. The introduction of  $Na_2WO_4$  into the base electrolyte influences the characteristics of electrolyte conductivity and the MAO process, and therefore, it is certain to influence the phase composition in the oxide coatings to some extent. However, the mechanisms responsible for the change of phase compositions in the oxide coating with addition of  $Na_2WO_4$  in base electrolyte need further detailed investigation.

The XPS specific spectrum of W4f for the oxide coating formed in silicate-KOH electrolytes with addition of 6.0 g/L  $Na_2WO_4$  is shown in Fig.5. This indicates that the  $WO_4^{2-}$  ions in the electrolyte incorporate into the coating during the MAO process. The spectrum can be identified well with two component peaks at around 36.3 eV and 31.4 eV, respectively. The one at around 36.3 eV corresponds to  $WO_3$  and/or  $Na_2WO_4$  and the other at around 31.4 eV is assigned to W element.

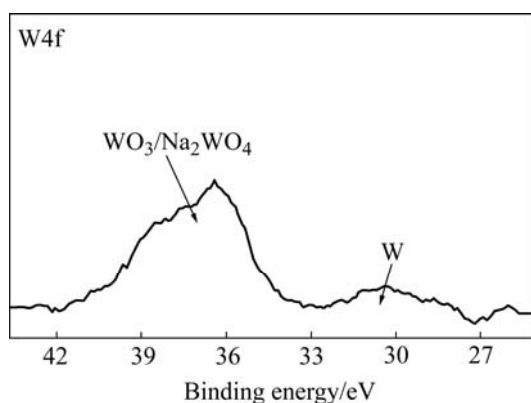


**Fig.5** XPS specific spectrum of W4f for oxide coating formed in silicate-KOH electrolyte with addition of 6.0 g/L  $Na_2WO_4$

During the MAO process, some of  $WO_4^{2-}$  ions are drawn into the discharges channels due to the strong electric field and a series of possible reactions take place for the incorporation of the  $WO_4^{2-}$  ions suggested by ZHENG et al[22]:



Due to an excess of Mg in the discharge channels, the reaction products  $WO_3$  react subsequently with Mg under a high-temperature condition by the following chemical reaction:



As a result, a trace amount of W element can be defined in the oxide coatings formed in electrolytes with addition of  $Na_2WO_4$  by XPS analysis. The fact that the oxide coatings formed in the electrolyte with addition of  $Na_2WO_4$  exhibit different colors may be contributed to

the presence of  $WO_3/Na_2WO_4$  and metallic W in the coatings (see Table 2).

### 3.3 Effect of $Na_2WO_4$ on mechanical and wear resistance properties of microarc oxidation coatings

The microhardness of the oxide coatings formed in different concentrations of  $Na_2WO_4$  is listed in Table 2. It can be seen that the microhardness of the oxide coatings increases gradually from HV 510 to HV 710 when the concentration of  $Na_2WO_4$  increases from 0 to 6.0 g/L. Different phase compositions of the coatings might account for the variation of microhardness of the oxide coatings. The XRD analysis reveals that the content of forsterite  $Mg_2SiO_4$  in the oxide coatings increases with increasing concentration of  $Na_2WO_4$  in the base electrolyte. Generally, forsterite  $Mg_2SiO_4$  has a greater hardness than periclase  $MgO$ [23]. As a result, the microhardness of the oxide coatings formed in electrolyte containing  $Na_2WO_4$  exhibits a higher value and increases with increasing concentration of  $Na_2WO_4$ .

The friction coefficients for the oxide coatings sliding against  $Si_3N_4$  ceramic ball under dry friction condition are also listed in Table 2. It is found that there are no significant differences in the friction coefficients for all the oxide coatings, which indicates that the addition of  $Na_2WO_4$  in the base electrolyte has little effect on the friction behavior of the oxide coatings. However, from Table 2 it can be seen that the wear rate of the oxide coatings decreases from  $3.55 \times 10^{-5} \text{ mm}^3/(\text{N}\cdot\text{m})$  to  $2.54 \times 10^{-5} \text{ mm}^3/(\text{N}\cdot\text{m})$  with increasing concentration of  $Na_2WO_4$  from 0 to 6.0 g/L in the base electrolyte, though the wear rates for all the oxide coatings maintain the same magnitude. This conforms to the variation of the content of the forsterite  $Mg_2SiO_4$  phase in the coatings. Because the concentration of  $Na_2WO_4$  influences the content of the forsterite  $Mg_2SiO_4$  phase in the coatings and then the microhardness influences eventually the wear performance of the coatings.

## 4 Conclusions

1) Oxide coatings are produced on AM60B magnesium alloys by microarc oxidation process in silicate-KOH electrolyte containing  $Na_2WO_4$ . The MAO process has a strong dependence on the concentration of  $Na_2WO_4$  and the breakdown voltage decreases from 200 to 135 V with increasing concentration of  $Na_2WO_4$  from 0 to 6.0 g/L in the base electrolyte.

2) With addition of  $Na_2WO_4$  into the base electrolyte the coating surface becomes more porous, the fraction of forsterite  $Mg_2SiO_4$  increases, a trace amount of metallic W forms in the oxide coatings and different

colors appear compared with that formed in the base electrolyte.

3) The microhardness of the oxide coatings increases; whereas the wear rates decrease with increasing concentration of  $\text{Na}_2\text{WO}_4$  in the base electrolytes because the content of the forsterite  $\text{Mg}_2\text{SiO}_4$  phase increases in the oxide coatings.

## References

- [1] MORDIKE B L, EBERT T. Magnesium: Properties—applications—potential [J]. *Mater Sci Eng A*, 2001, A302: 37–45.
- [2] YAMAUCHI N, DEMIZU K, UEDA N, CUONG N K, SONE T, HIROSE Y. Friction and wear of DLC films on magnesium alloy [J]. *Surface and Coatings Technology*, 2005, 193: 277–282.
- [3] GRAY J E, LUAN B. Protective coatings on magnesium and its alloys: A critical review [J]. *Journal of Alloys and Compounds*, 2002, 336: 88–113.
- [4] BARTAK D E, LEMIEUX B E, WOOLSEY E R. Hard anodic coating for magnesium alloys [P]. US 5470664, 1995.
- [5] ONO S, ASAMI K, OSAKA T, MASUKO N. Structure of anodic films formed on magnesium [J]. *Journal of Electrochemistry Society*, 1996, 143(3): L62–L63.
- [6] KHASELEV O, YAHALOM J. Constant voltage anodizing of Mg-Al alloys in  $\text{KOH-Al(OH)}_3$  solutions [J]. *Journal of Electrochemistry Society*, 1998, 145(1): 190–193.
- [7] BARTON B F, JOHNSON C B. The effect of electrolyte on the anodized finish of a magnesium alloy [J]. *Plating and Surface Finishing*, 1995, 82(5): 138–141.
- [8] YEROKHIN A L, NIE X, LEYLAND A, MATTHEWS A, DOWEY S J. Plasma electrolysis for surface engineering [J]. *Surface and Coatings Technology*, 1999, 122: 73–93.
- [9] YEROKHIN A L, LYUBIMOV V V, ASHITKOV R V. Phase formation in ceramic coatings during plasma electrolytic oxidation of aluminium alloys [J]. *Ceramics International*, 1998, 24: 1–6.
- [10] YEROKHIN A L, LEYLAND A, MATTHEWS A. Kinetic aspects of aluminium titanate layer formation on titanium alloys by plasma electrolytic oxidation [J]. *Applied Surface Science*, 2002, 200: 172–184.
- [11] YEROKHIN A L, NIE X, LEYLAND A, MATTHEWS A. Characterization of oxide films produced by plasma electrolytic oxidation of a Ti-6Al-4V alloy [J]. *Surface and Coatings Technology*, 2000, 130: 195–206.
- [12] RUDNEV V S, YAROVAYA T P, BOGUTA D L, TYRINA L M, NEDOZOROV P M, GORDIENKO P S. Anodic spark deposition of P, Me(II) or Me(III) containing coatings on aluminium and titanium alloys in electrolytes with polyphosphate complexes [J]. *Journal of Electroanalytical Chemistry*, 2001, 497: 150–158.
- [13] LIU J P, KUANG Y F. Microarc anodization technique and its development [J]. *Material Reviews*, 1998, 12(5): 27–29. (in Chinese)
- [14] BUTYAGIN P I, KHOKHRYAKOV Y V, MAMAEV A I. Microplasma systems for creating coatings on aluminium alloys [J]. *Mater Lett*, 2003, 57: 1748–1751.
- [15] LUKIYANCHUK I V, RUDNEV V S, KURYAVYI V G, BOGUTA D L, BULANOVA S B, GORDIENKO P S. Surface morphology, composition and thermal behavior of tungsten-containing anodic spark coatings on aluminium alloy [J]. *Thin Solid Films*, 2004, 446: 54–60.
- [16] WU X H, JIANG Z H, WANG F P, XIN S G, BENG H Q. Effect of potassium dichromate on structure and anticorrosive properties of ceramic film grown on Ti alloy by micro-plasma oxidation [J]. *The Chinese Journal of Nonferrous Metals*, 2001, 11(5): 806–809. (in Chinese)
- [17] GUAN Yong-jun, XIA Yuan. Correlation between discharging property and coatings microstructure during plasma electrolytic oxidation [J]. *Trans Nonferrous Met Soc China*, 2006, 16: 1097–1102.
- [18] IKONOPISOV S. Theory of electrical breakdown during formation of barrier anodic films [J]. *Electrochimica Acta*, 1977, 22: 1077–1082.
- [19] ALBELLA J M, MONTERO I, MARTINEZ-DUART J M. A theory of avalanche breakdown during anodic oxidation [J]. *Electrochimica Acta*, 1987, 32: 255–258.
- [20] XUE W, DENG Z, LAI Y, CHEN R. Analysis of phase distribution for ceramic coatings formed by microarc oxidation on aluminum alloy [J]. *Journal of American Ceramic Society*, 1998, 81: 1365–1368.
- [21] YEROKHIN A L, SNIZHKO L O, GUREVINA N L, LEYLAND A, PILKINGTON A, MATTHEWS A. Discharge characterization in plasma electrolytic oxidation of aluminium [J]. *Journal of Physics D: Applied Physics*, 2003, 36: 2110–2120.
- [22] ZHENG H Y, WANG Y K, LI B S, HAN G R. The effects of  $\text{Na}_2\text{WO}_4$  concentration on the properties of microarc oxidation coatings on aluminum alloy [J]. *Mater Lett*, 2005, 59: 139–142.
- [23] CAI Z Q, WANG L, YANG G. *Gradus of Ceramic Materials* [M]. Beijing: Chemical Industry Press, 2001: 171–326. (in Chinese)

(Edited by CHEN Wei-ping)